Int. J. Heat Mass Transfer. Vol. 14, pp. 1825–1834. Pergamon Press 1971. Printed in Great Britain.

CONDUCTIVITY EFFECTS ON RIBBED SURFACE HEAT TRANSFER

P. L. MANTLE, A. R. FREEMAN and J. WATTS

Central Electricity Generating Board, Berkeley Nuclear Laboratories, Gloucestershire, England

(*Received* 31 *August* 1970 *and in revised form* 15 *February* 1971)

Abstract—This paper considers heat-transfer from rib roughened surfaces, in particular A.G.R. fuel elements and the electrically heated scaled-up dummy elements used in establishing their performance in the Laboratory. It is shown that important corrections have to be made for the conductivity of the test element and coolant gas. Computed temperature distributions within ribbed surfaces are correlated in such a way that an allowance for surface heat-transfer efficiency (E_∞) can be predicted for different operating conditions. The laboratory heat-transfer measurements have to be reduced by typically 8 per cent to give performance information appropriate to reactor conditions. The principles should be applied to any heat-transfer surface when interpreting experimental results and comparing data.

NOMENCLATURE

A, area;
A_n, surface area of node n;
A_r, surface root area of roughened element i.e. area with ribs absent;
A_t, total surface area of roughened element;
B, Biot number;
B, B', modified Biot numbers;
C_p, specific heat;
E_∞, surface efficiency;
$G(r, z)$, function describing heat-transfer variation over a roughened surface;
Pr, Prandtl number;
Q, rate of heat-transfer/unit length;
R, dimensionless radius (r/ε);
Re, Reynolds number $(\rho v de/\mu)$;
St, Stanton number;
St_∞, Stanton number for an infinitely conducting surface;
T, temperature;
T_G, gas temperature;
T_i, inner wall temperature;
V, dimensionless temperature $(T-T_G)/(T_i-T_G)$;
Z, dimensionless length (z/ε);
de, equivalent diameter:
h, heat-transfer coefficient at point r, z on roughened surface;
h_a, mean heat-transfer coefficient over roughened surface;
h_e, effective heat-transfer coefficient as measured on a surface;
h_n, heat-transfer coefficient of node n;
k_g, thermal conductivity of gas;
k_m, thermal conductivity of metal;
n, refers to node n;
np, number of nodes in one rib pitch of surface;
q, surface flux at a point on a roughened surface;
q_n, surface flux at node n;
r, radius;
r_0, root radius of ribbed element;
t, wall thickness of roughened element;
v, fluid velocity;
w, rib width;
z, length;
ε, rib height;
ρ, density;
μ, fluid viscosity;
ΔT, maximum surface to gas temperature difference;
ΔT_∞, surface to gas temperature difference for $k_m = \infty$;
θ, angle.

INTRODUCTION

THE IMPROVEMENT in heat transfer caused by surface roughening has been studied for a considerable number of years. A roughened surface has been adopted for the stainless steel cladding of fuel pins in the Advanced Gas Cooled Reactors (A.G.R.).

Much of the development work for such a surface is carried out in the laboratory using relatively high conductivity aluminium test elements in a CO_2 loop operating at different conditions of temperature and pressure from those existing in the reactor.

Williams and Watts [1] have shown that for widely spaced rib type roughnesses, similar to those in the A.G.R., a very high heat-transfer coefficient exists over much of the rib and thus a high proportion of the heat passes through the rib. This means that there must be an axial flow of heat along or just below the surface of the test element. The proportion of heat flowing axially, for a given distribution of surface heat-transfer coefficient, will depend on the conductivity of the metal, the heat-transfer coefficient and, possibly the wall thickness between the ribs.

These effects have been investigated theoretically and numerically in this paper using published heat-transfer coefficient distributions. It is shown that the heat-transfer performance of a stainless steel surface operating under reactor conditions is typically 8 per cent lower than that of an aluminium surface tested under laboratory conditions. A generalized method of making a quantitative correction is given.

THEORY

The temperature distribution in the body of the roughened surfaces considered in this paper is determined by the conduction equation and the appropriate boundary conditions. The test elements and fuel pins can be assumed to be running under conditions of cylindrical symmetry so that variations of temperature with θ(in r, z, θ geometry) are zero. Thus,

$$\frac{\partial^2 T}{\partial r^2} + \frac{1}{r}\cdot\frac{\partial T}{\partial r} + \frac{\partial^2 T}{\partial z^2} = 0. \tag{1}$$

The heat-transfer coefficient between the roughened surface and the gas varies from place to place on the surface. However this variation $G(r, z)$ is often known and a heat-transfer coefficient h can be specified for every position on the roughened surface i.e.

$$h = h_a G(r, z) \tag{2}$$

where h_a represents the mean heat-transfer coefficient.

Also the bulk mean coolant gas temperature T_G can be specified as constant over one rib pitch.

The boundary condition at the element/gas interface may therefore be expressed in the form:

$$h(T - T_G) = -k_m \frac{\partial T}{\partial r}$$

$$\text{or } \frac{\partial T}{\partial r} + \frac{h_a G(r, z)}{k_m}(T - T_G) = 0. \tag{3}$$

Heat transfer from the rib sides may be considered similarly.

The boundary condition for the inner heated surface of the elements is assumed to be constant wall temperature i.e.

$$T = T_i = \text{constant}. \tag{4}$$

This is discussed later.

Equations (1), (3) and (4) determine the temperature distribution in the body of the test elements. These equations may be made dimensionless by defining dimensionless temperatures V in terms of a reference temperature difference $T_i - T_G$

$$V = \frac{T - T_G}{T_i - T_G}. \tag{5}$$

Similarly dimensionless lengths are defined in terms of the rib height ε.

$$R = \frac{r}{\varepsilon}$$

$$Z = \frac{z}{\varepsilon}.$$

Equation (1) becomes

$$\frac{\partial^2 V}{\partial R^2} + \frac{1}{R}\frac{\partial V}{\partial R} + \frac{\partial^2 V}{\partial Z^2} = 0. \quad (6)$$

Equation (3) becomes

$$\frac{\partial V}{\partial R} + \frac{\varepsilon h_a G(r, z)}{k_m}. V = 0. \quad (7)$$

Equation (4) becomes

$$V = 1. \quad (8)$$

Equations (6)–(8) completely define the temperature distribution within ribbed elements of the same dimensionless shape, i.e. constant P/ε, r_0/ε, t/ε, w/ε. Provided $G(r, z)$ is assumed to vary very little with changes in Reynolds number and Prandtl number, the temperature distribution solutions will only depend on the dimensionless group $\varepsilon h_a/k_m$. This is known as the Biot number.

The heat transfer performance of a ribbed element can be expressed in terms of E_∞ which is a measure of the surface efficiency.

It is defined

$$E_\infty = \frac{St}{St_\infty}$$

$$\text{or } E_\infty = \frac{\Delta T_\infty}{\Delta T}$$

where ΔT is the maximum element-gas temperature difference under the conditions of interest and ΔT_∞ the corresponding value under the same conditions of flux and heat-transfer coefficient but with the material conductivity assumed infinite

i.e.

$$\Delta T_\infty = \frac{\int\int qA\,\mathrm{d}r\,.\,\mathrm{d}z}{\int\int hA\,\mathrm{d}r\,.\,\mathrm{d}z}.$$

Thus for a particular geometry and heat-transfer coefficient distribution $G(r, z)$ the surface efficiency should be uniquely related to the Biot number. The aim of the next section is to calculate this relationship and show how to use it in the interpretation of experimental results.

METHOD OF ANALYSIS

The temperature distribution within the body of the ribbed test elements was calculated using the ORSFT 2 [2] computer program. This program solves the time dependant form of the heat conduction equation using a finite difference technique. The steady state solutions used in this paper were obtained by solving the equations successively until the rate of change of temperature was zero.

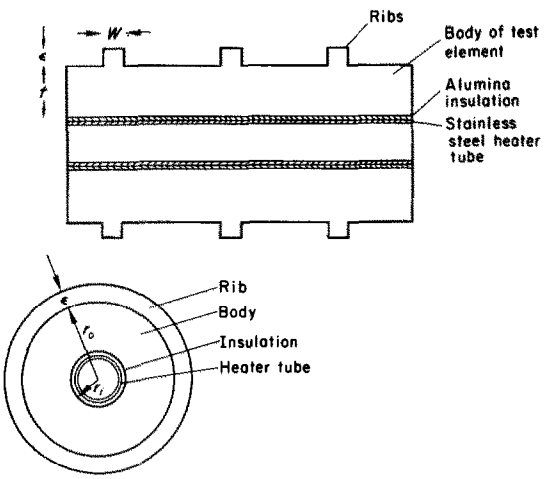

FIG. 1. A typical laboratory test element.

Figure 1 shows a typical test element which would be used in the laboratory to determine the heat-transfer performance of a particular ribbed surface. Figure 2 shows how the body of the element was divided up into "Nodes" for the ORSFT 2 analysis, which in this example is carried out in r, θ, z geometry with variations in the θ direction taken as zero.

For each example investigated the ORSFT 2 model was set up for a one rib pitch section of element. The nodes at opposite ends of the element were connected by the program to

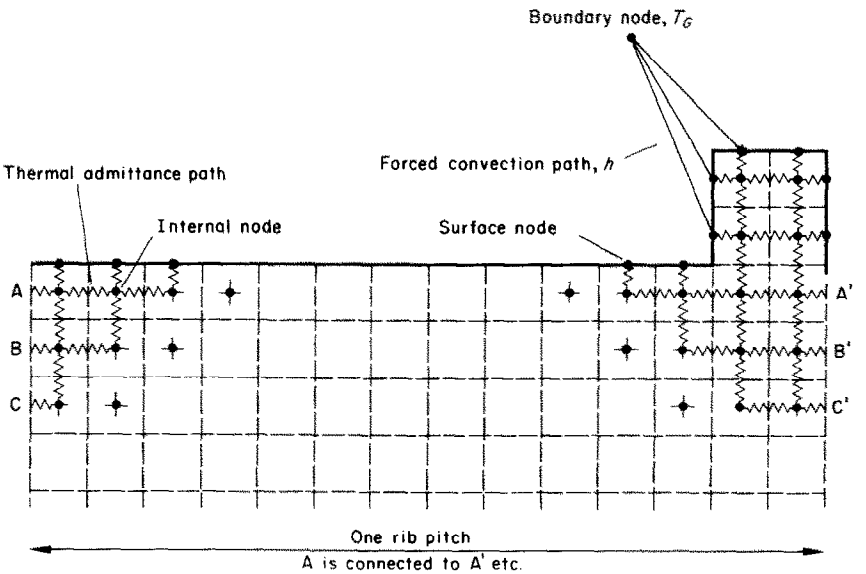

FIG. 2. Typical node structure used in roughened surface problems.

eliminate end conduction effects. A surface heat-transfer coefficient distributed as shown in Fig. 3 (Williams and Watts [1]) was assigned to the surface nodes. A coolant gas temperature and the heat source boundary conditions were also specified to correspond to various test conditions.

The output from ORSFT 2 is the temperature at each internal node and the heat flux and temperature at each surface node. This information is used to plot the isotherms within the element body (Fig. 4) and the distribution of surface temperature and flux (Fig. 5).

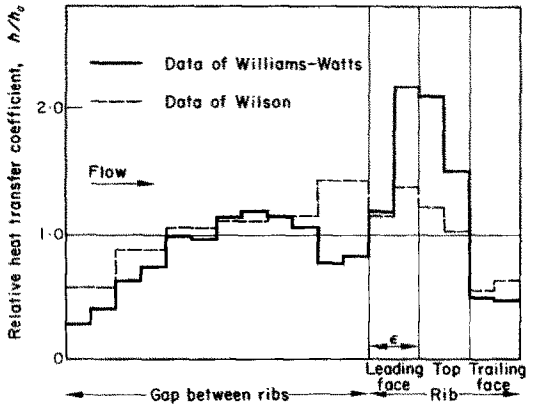

FIG. 3. The distribution of heat-transfer coefficient over ribbed heat-transfer surfaces.

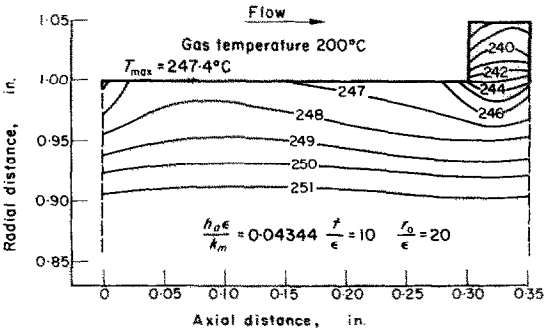

FIG. 4. Temperature distribution within the body of a roughened element.

The maximum can-to-gas temperature difference ΔT is determined from this figure, and ΔT_∞ is also readily determined from the ORSFT 2 output being given by:

$$\Delta T_\infty = \frac{\sum_1^{np} q_n A_n}{\sum_1^{np} h_n A_n}.$$

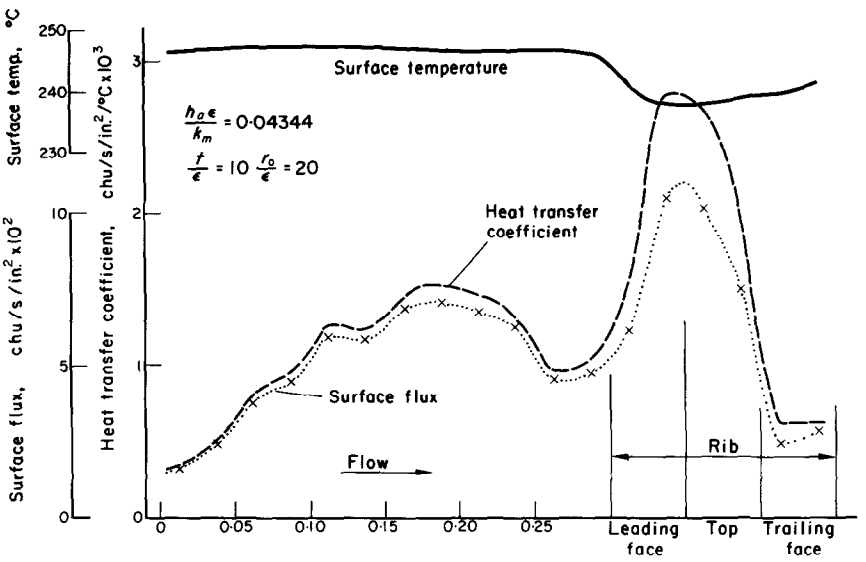

FIG. 5. Variation of surface temperature, surface heat flux and heat-transfer coefficient over a rib pitch of a roughened element.

Hence E_∞ was found:

$$E_\infty = \frac{\Delta T_\infty}{\Delta T}. \tag{9}$$

The Biot number corresponding to the test conditions was calculated from the input data

$$B = \frac{h_a \varepsilon}{k_m} \tag{10}$$

where h_a is the average surface heat-transfer coefficient and is given by

$$h_a = \frac{\sum_1^{np} h_n A_n}{\sum_1^{np} A_n}.$$

RESULTS

The analysis as described above was carried out for a variety of conditions. At first the geometry of the test element was maintained constant i.e. $P/\varepsilon = 7$, $w/\varepsilon = 1$, $t/\varepsilon = 10$, $r_0/\varepsilon = 20$, and a constant temperature inner wall boundary was used. The Biot number was varied by using a range of values of h_a, ε and k_m. The results are plotted in Fig. 6.

The effect of a substantial change in the distribution of the heat-transfer coefficient over the ribbed surface was studied by using the relatively flat heat-transfer coefficient distribution measured by Wilson [3] as shown in Fig. 3. For a given Biot number a higher E_∞ results as shown in Fig. 6.

All the above analyses were repeated using a constant flux inner wall boundary condition, and for the thick walled element considered, the same values of E_∞ were obtained as for the constant temperature case, see Fig. 6.

The effect of wall thickness (t/ε) was studied using both the constant temperature and constant flux inner wall boundaries. The results are presented in Fig. 7 for a constant Biot number.

Further runs were also carried out to represent a fuel can in a reactor with heat generated in the fuel pellets. Finally, since some laboratory experiments are performed using electrical resistance heating of the can wall itself a run was carried out to study this situation. The heat

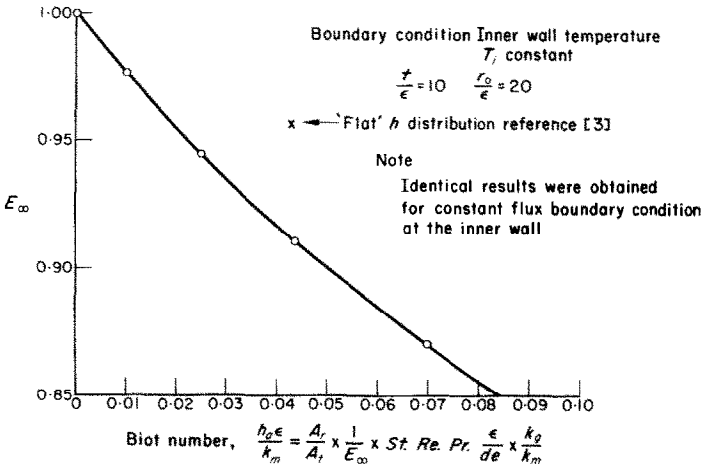

FIG. 6. The relationship between surface efficiency E_∞ and the surface Biot number $h_a\varepsilon/k_m$ for a thick walled element ($t/\varepsilon = 10$).

generation rate distribution within the ribbed can wall was computed using ORSFT 2 and the analogy between heat and electrical conduction. The temperature distribution within the wall was then found in the normal way using ORSFT 2, and hence E_∞ and the Biot number were calculated. The results for both the pellet heating and electrical wall heating are within 0·06 per cent of the constant inner wall flux case and are all shown as one line in Fig. 8 ($t/\varepsilon = 1{\cdot}36$).

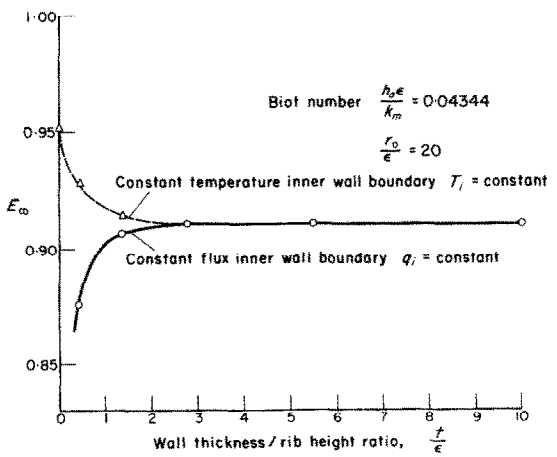

FIG. 7. Surface efficiency, E_∞, as a function of the wall thickness–rib height ratio for both constant flux and constant temperature boundary conditions.

APPLICATION OF RESULTS

In a laboratory experiment the maximum can-to-gas temperature difference ΔT_{max} and the heat rating are the usual quantities measured and from these an effective heat-transfer coefficient h_e and Stanton number are determined based on the root surface area A_r. If Q is the rate of heat-transfer, then

$$Q = h_e \cdot A_r \cdot \Delta T_{max} \tag{11}$$

$$\text{and } St = \frac{h_e}{C_p \cdot \rho \cdot v}.$$

From equations (9) and (11), therefore, the rate of heat-transfer can be represented by:

$$Q = h_e \cdot A_r \cdot \frac{\Delta T_\infty}{E_\infty}. \tag{12}$$

Since h_a is the average heat-transfer coefficient over the total surface area A_t, the heat rate can also be represented by:

$$Q = h_a \cdot A_t \cdot \Delta T_\infty. \tag{13}$$

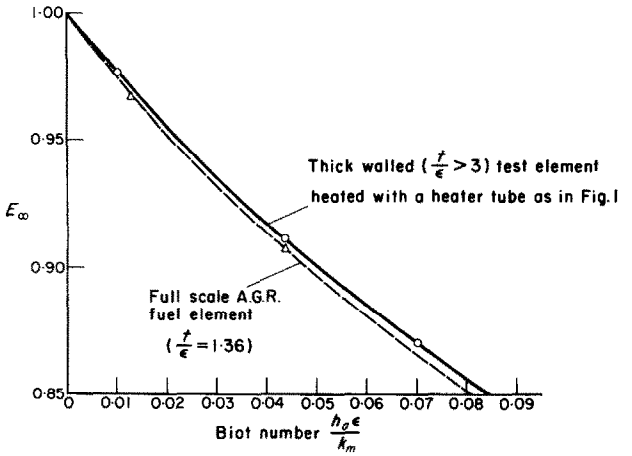

FIG. 8. Surface efficiency, E_∞ as a function of the surface Biot number $h_a\epsilon/k_m$ for typical reactor fuel pins and laboratory test elements.

Hence, using the equations (10), (12) and (13), the Biot number may be written:

$$B = \frac{A_r}{A_t}.\frac{1}{E_\infty}.\frac{h_a\varepsilon}{k_m}$$

$$\text{or } B = \frac{A_r}{A_t}.\frac{1}{E_\infty}.St\,.Re\,.Pr\,.\frac{\varepsilon}{de}.\frac{k_g}{k_m}.$$

However, for most practical purposes, this expression is not the most convenient, and so that E_∞ may be found explicitly, use is made of modified Biot numbers, B' and B'', where:

$$B' = St\,.Re\,.Pr\,.\frac{\varepsilon}{de}.\frac{k_g}{k_m}$$

$$\text{and } B'' = St_\infty\,.Re\,.Pr\,.\frac{\varepsilon}{de}.\frac{k_g}{k_m}$$

On the basis of these parameters, Figs. 9 and 10 are plotted from the data presented in Fig. 8.

The Stanton number for experimental conditions, St_1, can now be corrected as outlined

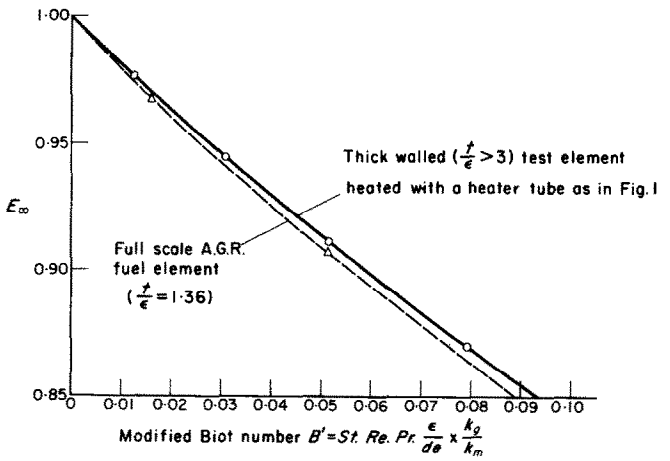

FIG. 9. Surface efficiency E_∞ as a function of the modified Biot number, B'.

below, so as to provide the Stanton number, St_2, for some other conditions, e.g. reactor conditions.

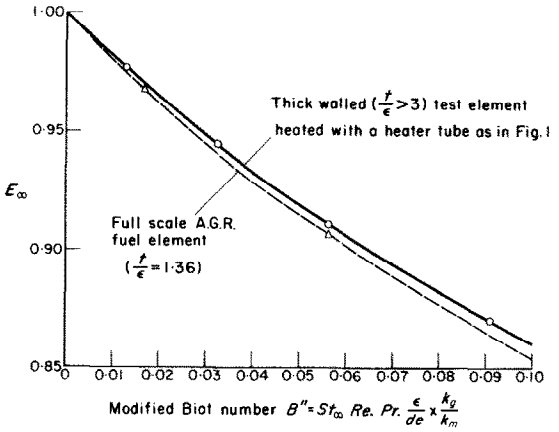

FIG. 10. Surface efficiency E_∞ as a function of the modified Biot number, B''.

The experimental data, St_1, Re, Pr, ε/de and k_g/k_m are used in Fig. 9 to determine a value of E_∞, say $E_{\infty 1}$, which applies to the experimental conditions, and hence $St_{\infty 1}$ is found,

$$St_{\infty_1} = \frac{St_1}{E_{\infty_1}}.$$

Now, assuming comparisons are made at the same values of Reynolds number and ε/de, and that the following relationship holds,

$St \propto Pr^{-0.6}$

then St_{∞_2} is given by

$$St_{\infty_2} = St_{\infty_1}\left(\frac{Pr_1}{Pr_2}\right)^{0.6}.$$

The reactor data and St_{∞_2} are now used to calculate B'', enabling E_{∞_2} to be evaluated from Fig. 10.

The performance of the surface at reactor conditions, St_2, is now given by:

$$St_2 = St_{\infty_2} \times E_{\infty_2}.$$

For conditions (1)

$$B' = St_1 . Re . Pr . \varepsilon/de . k_g/k_m = 0{\cdot}0028$$

Example

	Laboratory data (1)	Reactor data (2)
Material coolant	Aluminium CO_2(200°C)	Stainless steel CO_2(600°C)
ε/de	0·007	0·007
t/ε	10	1·36
k_g CHU/in.s °C	$4{\cdot}15 \times 10^{-7}$	$8{\cdot}0 \times 10^{-7}$
k_m CHU/in.s °C	$3{\cdot}1 \times 10^{-3}$	$3{\cdot}25 \times 10^{-4}$
Re	8×10^5	8×10^5
Pr	0·7464	0·7265
St	0·005	

hence $E_{\infty 1} = 0{\cdot}994$ from Fig. 9 for a $t/\varepsilon = 10$

$$\therefore St_{\infty_1} = \frac{0{\cdot}005}{0{\cdot}994}.$$

Therefore for conditions (2)

$$St_{\infty_2} = \frac{0{\cdot}005}{0{\cdot}994}\left(\frac{0{\cdot}7464}{0{\cdot}7265}\right)^{0.6}$$

$$= 0{\cdot}005113.$$

$$\text{Now } B'' = St_{\infty_2}\, Re\, Pr\, \varepsilon/de\, k_g/k_m$$

$$= 0{\cdot}05120.$$

Hence from Fig. 10 $E_{\infty_2} = 0{\cdot}914$ for $t/\varepsilon = 1{\cdot}36$

$$\therefore St_2 = 0{\cdot}005113 \times 0{\cdot}914$$

$$= 0{\cdot}00467.$$

The Stanton number under reactor conditions will therefore be 6·5 per cent lower than the value measured in the laboratory.

DISCUSSION

The theory demonstrates that the Biot number governs the temperature distribution in a ribbed heat-transfer surface for a given geometry and heat-transfer coefficient distribution. A constant temperature inner wall boundary condition is assumed, but a similar result could have been derived using constant flux or some other heat source boundary condition.

The results of the numerical analysis plotted in Fig. 6 show that if the same Biot number is

achieved using different values of h_a, ε, and k_m then the same E_∞ is obtained. This confirms that the temperature field, or rather a particular feature of it E_∞, is uniquely related to the Biot number for a given distribution of heat-transfer coefficient over the surface and constant pin wall geometry with a specified heat source boundary condition.

The heat-transfer coefficient distribution over the ribbed surface was taken from the data of Williams and Watts [1] (see Fig. 3) who used a water vapour mass transfer analogue. These results are very similar to the earlier work of Kattchee and Mackewicz [4] and to the results of Wilkie [5] who both used a naphthalene sublimation technique. However Wilson [3] reported a much flatter distribution with relatively low coefficients over the rib top. This is regarded as non-typical and is used to show the effect of a substantial change in the distribution of the heat-transfer coefficient, see Fig. 6. As expected the flatter distribution gives E_∞ values closer to unity than those obtained from a more typical distribution. In general very little variation in the distribution has been reported even when considerable changes have been made in the Reynolds number.

The results presented in Fig. 7 show that the effect of reducing wall thickness (t/ε) depends on what heat source boundary condition is applied. Below a t/ε value of about 3, E_∞ increases with decreasing wall thickness if the boundary condition applied is that of constant temperature, whereas for constant flux E_∞ is seen to decrease.

At a value for t/ε of 1·36, which is typical for reactor fuel cans, the discrepancy is only about 0·8 per cent, but below this value the two lines diverge very rapidly to limiting values for E_∞ of 0·952 in the case of constant temperature, and 0·216 in the case of constant flux.

It is obvious from Fig. 7 why the results of the initial investigation, for a t/ε value of 10, were identical for the two different boundary conditions.

The remainder of the runs, to establish the effect of different modes of heating, were mostly performed at $B = 0{\cdot}04344$ and $t/\varepsilon = 1{\cdot}36$, these being typical reactor values. The results show at this Biot number that the effect of changes in the heat source on E_∞ are very small indeed. In both the case of fuel pellet heating, and where the heat was generated electrically in the can wall itself, the results correspond to within 0·06 per cent of that obtained using a constant inner wall heat flux boundary condition. Since the differences are so small it is not possible to distinguish between the modes of heating in Fig. 8, and therefore the results for a 'reactor type can' are shown by a single dashed line.

In the laboratory heat may be sometimes supplied from an electrically heated tube sprayed with alumina insulation which is then mounted in the bore of the test element as in Fig. 1. The inner wall boundary condition will be somewhere between constant temperature and constant flux. However since the wall thickness of such elements is usually greater than $t/\varepsilon = 3$ the type of boundary condition will have no effect and the E_∞ values will be as in Fig. 6. These are shown by a full line in Fig. 8.

All the results presented in this paper apply to cases where the radius of the test element is large compared with the rib size i.e. $r_0/\varepsilon = 20 \rightarrow 28$. Should small values of r_0/ε ever be of interest then new E_∞ – Biot curves would have to be derived.

As the example shows, the correction from laboratory to reactor conditions for conductivity effects can be very significant. The conductivity effects alone produce a -8 per cent correction and a Prandtl number change gives a $+1{\cdot}6$ per cent correction resulting in a nett $-6{\cdot}5$ per cent. The graphs of E_∞ v. modified Biot numbers presented in Figs. 9 and 10 are very convenient for calculating the corrections.

CONCLUSIONS

The importance of thermal conductivity effects in the interpretation of the heat-transfer performance of ribbed surfaces is demonstrated.

A simple method of making corrections for a particular type of ribbed surface is given. The principles are generally applicable to all heat-transfer surfaces.

ACKNOWLEDGEMENT

This paper is published by permission of the Central Electricity Generating Board.

REFERENCES

1. F. WILLIAMS and J. WATTS, The development of rough surfaces with improved heat transfer performance and a study of the mechanisms involved, F.C. 5.5, Fourth International Heat Transfer Conference, Paris (1970).
2. A. LICKORISH, ORSFT 2—A revised version of the IBM 7090 program ORSIFT for computing heat distributions, CEGB/RD/C/M12.
3. J. WILSON, Mass transfer tests on roughened surfaces, Private communication U.K.A.E.A., Windscale Laboratory (1968).
4. N. KATTCHEE and W. MACKEWICZ, Effects of boundary layer turbulence promoters on the local film coefficients of ML-1 fuel elements, *Nucl. Sci. Engng* **16**, 31–38 (1963).
5. D. WILKIE, Forced convection heat transfer from surfaces roughened by transverse ribs, Paper 1, 3rd International Heat Transfer Conference, Chicago (1966).

EFFETS DE CONDUCTIVITE SUR LE TRANSFERT THERMIQUE D'UNE SURFACE CANNELEE

Résumé—Cet article concerne le transfert thermique des surfaces rugueuses cannelées, en particulier des éléments combustibles A.G.R. et des éléments modèles chauffés électriquement utilisés pour déterminer en laboratoire leurs performances. On montre que des corrections importantes doivent être faites pour la conductivité de l'élément d'essai et le gaz réfrigérant. Des distributions de température calculées pour surfaces cannelées sont regroupées de manière à prédire l'efficacité thermique de la surface (E_∞) pour différentes conditions opératoires. Les mesures thermiques sont unifiées à 8 pour cent près et donnent une information appropriée sur les performances dans les conditions du réacteur. Les principes peuvent être appliqués à une surface quelconque à partir d'essais comparatifs et des résultats expérimentaux d'interprétation.

WÄRMELEITEFFEKTE BEIM WÄRMEÜBERGANG AN BERIPPTEN OBERFLÄCHEN

Zusammenfassung—Diese Arbeit behandelt den Wärmeübergang an berippten Oberflächen, insbesondere an A.G.R.-Brennstoffelementen und an vergrösserten, elektrisch beheizten Vergleichselementen, wie sie für Laborversuche verwendet wurden.

Es wird gezeigt, dass erhebliche Korrekturen zu machen sind für die Leitfähigkeit des Testelements und des Kühlgases. Berechnete Temperaturverteilungen in berippten Flächen werden so korreliert, dass für verschi dene Betriebsbedingungen ein Bereich für den Wärmeübergang an der Oberfläche angegeben werden kann. Die Wärmeübergangsmessungen im Laboratorium müssen um 8% verkleinert werden, um Informationen für den Betrieb unter Reaktorbedingungen zu liefern. Dieses Verfahren sollte auf den Wärmeübergang an beliebigen Oberflächen angewendet werden, wenn man experimentelle Ergebnisse und Vergleichsdaten auswerten will.

ВЛИЧНИЕ ТЕПЛОПРОВОДНОСТИ НА ОРЕБРЕННЫЕ ПОВЕРХНОСТИ ТЕПЛООБМЕНА

Аннотация—В статье рассматривается теплообмен от оребренных шероховатых поверхностей, в частности в топливных элементах и нагреваемых электричеством крупномасштабных моделях элементов, используемых для определения их рабочих характеристик в лабораторных условиях. Показано, что необходимо внести поправку на теплопроводность испытуемого элемента и газообразного охладителя. Рассчитанные распределения температуры внутри оребренных поверхностей обобщаются таким образом, что можно учесть эффективность поверхностного теплообмена (E_∞) для различных рабочих условий. Лабораторные измерения теплообмена необходимо уменшить обычно на 8% для того, чтобы получить данные по характеристикам, соответствующим условиям реактора. Эти принципы должны применяться к любой поверхности теплообмена при обработке экспериментальных результатов и сравнении данных.